AIP | Review of Scientific Instruments

Bandwidth-variable tunable optical filter unit for illumination and spectral imaging systems using thin-film optical band-pass filters

Georg Hennig, Gary M. Brittenham, Ronald Sroka, Gesa Kniebühler, Michael Vogeser, and Herbert Stepp

Citation: Review of Scientific Instruments **84**, 043113 (2013); doi: 10.1063/1.4803003
View online: http://dx.doi.org/10.1063/1.4803003
View Table of Contents: http://scitation.aip.org/content/aip/journal/rsi/84/4?ver=pdfcov
Published by the AIP Publishing

Bandwidth-variable tunable optical filter unit for illumination and spectral imaging systems using thin-film optical band-pass filters

Georg Hennig,[1,a)] Gary M. Brittenham,[2] Ronald Sroka,[1] Gesa Kniebühler,[1] Michael Vogeser,[3] and Herbert Stepp[1]

[1]*Laser-Forschungslabor, LIFE Center, Klinikum der Universität München, Marchioninistr. 23, 81377 München, Germany*

[2]*Division of Pediatric Hematology, Oncology and Stem Cell Transplant, Department of Pediatrics, Columbia University College of Physicians and Surgeons, 3959 Broadway, New York, New York 10032, USA*

[3]*Institute of Laboratory Medicine, Klinikum der Universität München, Marchioninistr. 15, 81377 München, Germany*

(Received 7 March 2013; accepted 12 April 2013; published online 30 April 2013)

An optical filter unit is demonstrated, which uses two successively arranged tunable thin-film optical band-pass filters and allows for simultaneous adjustment of the central wavelength in the spectral range 522–555 nm and of the spectral bandwidth in the range 3–16 nm with a wavelength switching time of 8 ms/nm. Different spectral filter combinations can cover the complete visible spectral range. The transmitted intensity was found to decrease only linearly with the spectral bandwidth for bandwidths >6 nm, allowing a high maximum transmission efficiency of >75%. The image of a fiber bundle was spectrally filtered and analyzed in terms of position-dependency of the transmitted bandwidth and central wavelength. © *2013 AIP Publishing LLC*. [http://dx.doi.org/10.1063/1.4803003]

I. INTRODUCTION

Optical filtering is a common task in laboratory or clinical light applications such as illumination and detection systems,[1] e.g., for fluorescence spectroscopy. It is also necessary for spectral imaging,[2,3] e.g., for filtering images from fiber bundles used in endoscopy or for fluorescence microscopy. Often, it is desired to be able to quickly switch between different central wavelengths at a small spectral bandwidth, without requiring tunable lasers or other expensive equipment. Diffraction-based monochromators, e.g., Czerny-Turner type grated monochromators,[4] are commonly used for non-imaging spectrometers.[1,2] For this type of monochromator, the transmitted intensity decreases with decreasing bandwidth in a greater than linear manner that is approximately proportional to the square of the bandwidth for a given light source diameter,[1] limiting its applicability to high intensity illumination systems. For spectral imaging, diffraction-based monochromators require a scanning unit,[2] which is a limitation that can be overcome by using other filter types such as acousto-optic tunable filters,[2,5,6] linear variable optical filters,[2,5,7,8] or liquid-crystal tunable filters.[2,5,9,10] For most of these filter types, however, either bandwidth or central wavelength can be adjusted, but not both,[6,11] the tuning range of the bandwidth or central wavelength may be limited,[7,12] or the transmission characteristics depend on the position of the incident light on the filter.[7,8]

Cholesteric liquid crystals (CLCs) exhibit reflection properties that depend on the angle of incidence, polarization, electrical or magnetic field, temperature, radiation, or mechanical pressure.[13–18] CLCs were used to demonstrate optical filter units that allow for simultaneous adjustment of the central wavelength and spectral bandwidth.[15,16] The polarization-dependent reflection efficiency limits the transmission efficiency of these demonstrated filter units to less than 45%,[15,16] which may be improved by combining crystals with different polarization dependency.[16] However, for these filter units, light suppression outside the transmitted pass-band is limited.[15,16] When tuning the wavelength by the angle of incidence, the transmitted beam of light is displaced due to the reflection geometry, making optical alignment cumbersome.[15,16] This is not the case when tuning the filters by temperature adjustment[16] instead of rotating the filters. Nonetheless, temperature adjustment is time consuming and therefore yields only a slow tuning speed of 0.39 s/nm.[16]

An optical filter unit that overcomes some of these limitations uses the same concept of independent adjustment of overlapping filter pass-bands:[15,19] two commercially available thin-film optical band-pass filters in a transmission setup[12,19] are successively arranged for simultaneous adjustment of both the central wavelength and the transmission bandwidth. A single tunable thin-film filter shows a transmission efficiency of more than 90% in the pass-band,[5] whose central wavelength shifts upon rotation of the filter. The spectral bandwidth remains virtually constant and, in particular, is independent of the polarization of the transmitted light,[3,5,19] so that the transmission efficiency in the pass-band remains virtually constant as well. If two such filters are arranged successively, an independent rotation of the filters to different angles spectrally shifts the filter pass-bands against each other, and light is transmitted through the filter unit only in the spectral range where the filter pass-bands overlap. Even when tuning the filter unit to different central wavelengths with a fixed bandwidth, the two filters must be rotated independently due to the nonlinear relation between the central wavelength

a)Author to whom correspondence should be addressed. Electronic mail: georg.hennig@med.lmu.de. This paper is part of the inaugural thesis of Georg Hennig to be submitted at the Medical Faculty of the Ludwig-Maximilians-Universität.

of the transmitted pass-band and the angle of incidence, compare Eq. (1) and Fig. 3. In contrast to reflection filters,[15] no angular deviation occurs when rotating the filters, moreover preserving the fast tuning speed of the filter unit that is tuned by the angle of incidence.[15] A parallel beam shift occurs when light passes through the rotated filters,[19] which may be compensated at least partly by rotating the filters in opposite directions, so that the beam shifted by the first filter is partly shifted back by the second filter. The maximum transmission efficiency is found in the center of the spectral range where the filter pass-bands overlap. This maximum transmission efficiency equals the product of the transmission efficiencies of both filters at their respective spectral positions. Therefore, if both filters show high transmission efficiency in the overlapping pass-band, the product of the two transmission efficiencies is high and independent of the bandwidth of the overlapping spectral range. However, to achieve a very small bandwidth, only the edges of the two filter pass-bands overlap. In this case, the maximum transmission efficiency is lower. Altogether, the transmission efficiency of the filter unit can be expected to not depend on the bandwidth, as long as the minimal achievable bandwidth is not limited by the filter edge steepness. The transmitted intensity of light depends on the area under the total transmitted pass-band that decreases in this case only linearly with the optical bandwidth in contrast to diffraction-based monochromators, indicating the applicability of the filter unit to high intensity illumination systems. Additionally, the band-pass filters used in the demonstrated filter unit are, in principle, capable of filtering images without the need of scanning units.[3,12] This can be done by filtering the image in a collimated beam.[12] However, photons from different positions in the focal plane show different divergence angles in the collimated beam and therefore different angles of incidence on the rotated filters. These differences lead to different spectral shifts of the filter pass-bands, so that the filtering characteristics of the filter unit can be assumed to depend on the position of the light source within the focal plane. The remaining divergence angle of a collimated beam is smaller for a larger focal width, so that the filtering characteristics of the filter unit can also be assumed to depend on the focal width of the collimating lens.

In this study, a filter unit combining two identical tunable thin-film optical band-pass filters with their pass-bands in the green wavelength range (central wavelength tuning range: 502–561 nm) is analyzed. To evaluate its applicability to high intensity illumination systems, white light from a 1500 μm core diameter fiber is spectrally filtered by the filter unit and coupled again into a 1500 μm core diameter fiber. The transmission characteristic of one filter is compared to the filter specifications and to the transmission achieved by the complete filter unit, consisting of two identical filters. The limits of the achievable tuning range and bandwidth variation are evaluated. The limitations of the filter unit when filtering images are demonstrated by filtering the collimated beam from 7 linearly arranged 200 μm core diameter fibers, comparing collimating lenses with different focal lengths, and measuring the spectrum of the transmitted light for each fiber for different directions of rotation of the filters.

II. MATERIAL AND METHODS

A. Tunable thin-film optical band-pass filters

Two tunable thin-film optical band-pass filters (561/14 nm VersaChrome®, Semrock, Inc., Rochester, NY, USA, filter size 25.2 mm × 35.6 mm × 2.0 mm, central wavelength $\lambda_C = 561$ nm at perpendicular angle of incidence $\theta = 0°$, and the effective refractive index $n_{eff} = 1.83$), were implemented for spectral filtering. The central transmission wavelength λ_C of the filters depends on the angle of incidence θ of the light beam relative to the surface normal of the filter and on the effective refractive index n_{eff}, which is particular for the tunable band-pass filter that is used. The angular dependency of λ_C can be described[3,5] by

$$\lambda_C(\theta) = \lambda_C(0)\sqrt{1 - \frac{\sin^2\theta}{n_{eff}^2}}. \quad (1)$$

B. Experimental setup

As shown schematically in Fig. 1(a), white light from a short-arc Xe-lamp (D-Light, Karl Storz GmbH & Co. KG, Tuttlingen, Germany) was coupled into a 1500 μm core diameter fiber (NA = 0.35, Karl Storz GmbH & Co. KG, Tuttlingen, Germany), referred to as the "source fiber." The white light from the source fiber was collimated by an aspherical condenser lens (D = 22.4 mm, f = 18 mm, LINOS system, Qioptiq Photonics GmbH & Co. KG, Göttingen, Germany), referred to as "collimating lens," with a remaining divergence angle of 2.1° of the collimated beam. Then, the collimated beam of white light passed through the two tunable thin-film optical band-pass filters, with the optical axis adjusted to the

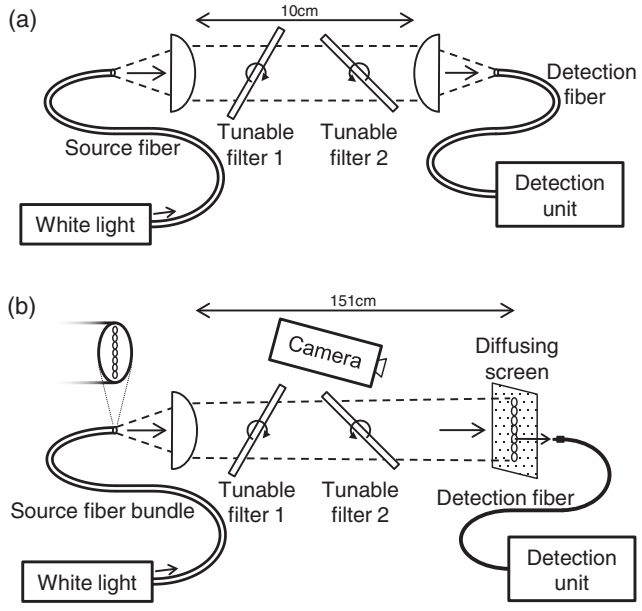

FIG. 1. Schematic of the measurement setup. (a) White light transmitted through a source fiber (1500 μm core diameter) is filtered by two independently tunable optical filters. The detection unit consists of a detection fiber (1500 μm core diameter), which is coupled into a CCD spectrometer. (b) A fiber bundle with 7 linearly arranged fibers (200 μm core diameter) served as source fiber, and the image of the fiber bundle on a diffusing screen is recorded by a camera. The spectrum of each fiber is acquired by the spectrometer.

center position of the filters. The filter mounts were coupled to two stepper motors (Nanotec Electronic GmbH & Co. KG, Landsham, Germany) so that they could be rotated individually using stepper motor controllers (SMCI32, Nanotec Electronic GmbH & Co. KG, Landsham, Germany), which were actuated by a custom interface (LabVIEW, National Instruments Corporation, Austin, TX, USA). One step equaled 1.8° with 16 microsteps per step, yielding an angular increment of 0.1125° per microstep. The time required for rotating a filter from $\theta = 0°$ to $\theta = 51°$ was 400 ms, yielding an effective response time of 8 ms/nm. Both filters could be removed independently from the filter unit to perform measurements either without or with one or two tunable filters. The filters could be rotated individually clockwise or counterclockwise, yielding rotation in opposite directions ("counter-directional") or the same direction ("equidirectional"). The parallel beam shift that occurs, when the collimated beam of light passes through the 2 mm thick filters rotated to different angles, can be estimated by theoretical considerations to be less than 200 μm for counter-directional rotation, while for equidirectional rotation, it is less than 1200 μm. After transmission through the filter unit (length: 10 cm, compare Fig. 1(a)), the filtered collimated beam of light was then focused by the "focusing lens," which was identical to the collimating lens, and focused onto a 1500 μm core diameter fiber (NA = 0.48, CeramOptec GmbH, Bonn, Germany), referred to as the "detection fiber." For spectrally resolved detection, the detection fiber was coupled into the detection unit, where the spectrum was detected by a CCD spectrometer (2048 pixel, 339-1029 nm, USB2000+, OceanOptics, Inc., Dunedin, FL, USA) with an effective spectral resolution of 2 nm.

To demonstrate the filter unit's ability to filter images, the image of a fiber bundle, consisting of 7 linearly arranged fibers (200 μm core diameter each, NA = 0.22, LightGuideOptics Germany GmbH, Rheinbach, Germany), was displayed on a reflecting diffusing screen (TiO_2 coated), which was located at a distance of 151 cm from the collimating lens, as shown schematically in Fig. 1(b). The axis along which the fibers were arranged was perpendicular to the filter rotation axis. The collimated 7 beams transmitted through the filter unit had a remaining divergence half angle of 2.6°. The image of the fiber bundle was recorded by a consumer grade camera (Ixus 970 IS, Canon, Inc., Tokyo, Japan). Additionally, the spectrum of the image of each fiber was acquired by the detection unit using a 50 μm core optical fiber (NA = 0.22, Thorlabs, Inc., Newton, NJ, USA).

To demonstrate the influence of the focal length of the collimating lens on the total transmission efficiency, the collimating lens with f = 18 mm was replaced by another aspherical condenser lens with f = 27 mm (D = 31.5 mm, LINOS system, Qioptiq Photonics GmbH & Co. KG, Göttingen, Germany), resulting in a reduced divergence half angle of 1.5° of the collimated beam.

C. Evaluation

The evaluation and graphical presentation of the recorded spectra was performed by MATLAB (R2012a, MathWorks®, Natick, MA, USA). First, a dark spectrum was subtracted from each recorded spectrum. The resulting spectrum was calibrated for the wavelength-dependent spectrometer sensitivity, yielding the calibrated "filtered spectrum." The evaluation of the transmission efficiency through one or two filters was performed by dividing the "filtered spectrum" by the spectrum of the light coupled into the detection fiber without any filter, yielding the "transmission spectrum." The maximum of this transmission spectrum was identified and is referred to as the "maximum transmission efficiency."

The evaluation of the spectral bandwidth of the transmitted pass-band was performed by first identifying the maximum intensity of the "transmission spectrum" and thereafter by iterating through the pixel values from the lowest and highest recorded wavelength towards the maximum and identifying the two spectral positions at each side of the pass-band, where the intensity was 50% of the maximum intensity, and finally by interpolating linearly between the two neighboring pixels in the spectrum. The resulting spectral width is referred to as the "spectral bandwidth" λ_{SB} (full width at half maximum, FWHM). The "central wavelength" λ_C of the transmitted pass-band was evaluated by calculating the center position between the two spectral positions at each side of the pass-band where 50% of the maximum intensity was reached. In a similar way, the edge steepness was quantified by evaluating the difference of the spectral positions, where 10% and 90% of the maximum intensity was reached, and averaging over both sides of the transmitted pass-band. The "transmitted intensity" was evaluated by calculating the sum over all pixels of the transmission spectrum within the spectral range 490–580 nm to cover the pass-band for the whole tuning range.

III. RESULTS

A. Single filter

In Fig. 2, the filtered spectrum of one filter at different filter angles θ is shown, relative to the transmitted light without any filter. The central wavelength λ_C shifts towards smaller wavelengths at increasing angles, while the spectral

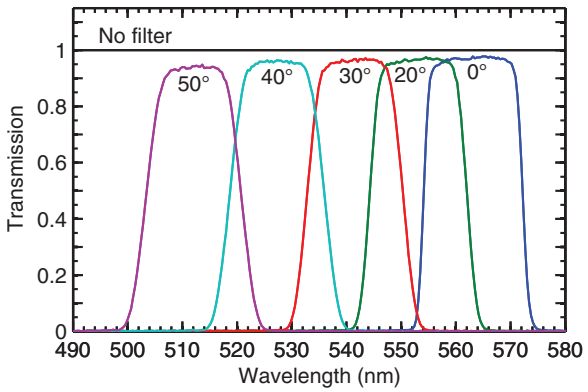

FIG. 2. The transmission spectrum, relative to the transmission without any filter, is shown for the setup in Fig. 1(a) with one tunable thin-film optical band-pass filter inserted at the filter rotation angles θ = [0°, 20°, 30°, 40°, 50°] shown below each transmission spectrum, with λ_C = [563.2 nm, 553.2 nm, 541.6 nm, 527.2 nm, 512.0 nm] and λ_{SB} = [18.1 nm, 17.8 nm, 17.6 nm, 17.4 nm, 17.5 nm].

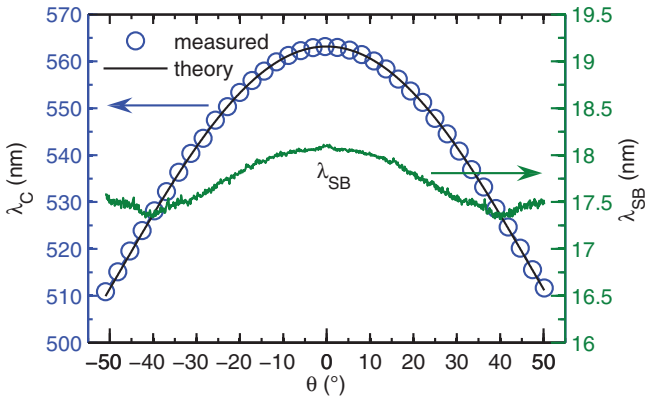

FIG. 3. The central wavelength λ_C (left y-axis) and bandwidth λ_{SB} (right y-axis) of the transmission spectrum using one tunable thin-film optical band-pass filter at different angles are shown, as well as the theoretically predicted central wavelength. The bandwidth varies only between 17.3 and 18.1 nm, while the central wavelength could be tuned between 510 nm and 563 nm.

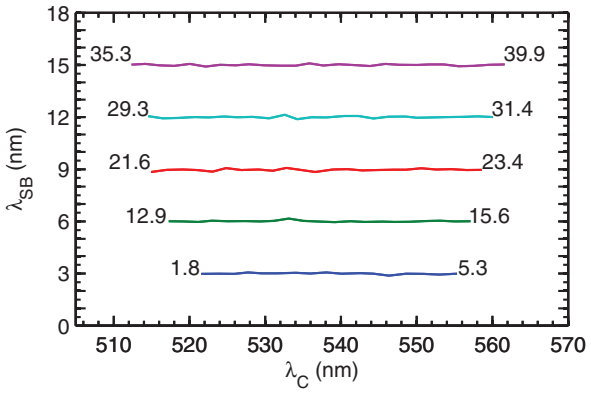

FIG. 5. The bandwidth of the transmitted light is plotted as a function of the transmitted central wavelength for five bandwidth settings, 3–15 nm (3 nm increments), demonstrating the freely adjustable central wavelength at defined bandwidth settings. The tuning range is limited by the bandwidth setting (maximum bandwidth setting range: 3 nm $\leq \lambda_{SB} \leq$ 16 nm). The transmitted intensity in arbitrary units is denoted for each bandwidth setting at the highest and lowest achievable central wavelength λ_C.

bandwidth λ_{SB} of the transmitted light remains virtually constant, although with flattened edges of the pass-band at increasing θ and decreasing λ_C (edge steepness: 2.1 nm for $\theta = 0°$, 5.3 nm for $\theta = 50°$). From the transmission spectrum, the maximum transmission efficiency was evaluated, being larger than 97% for $\theta = 0°$, and still larger than 94% for $\theta = 50°$.

The quantitative results of λ_C and λ_{SB} of the transmission pass-band of one filter at different θ are shown in Fig. 3. The measured λ_C follows the theoretical prediction of Eq. (1). By rotating the filter from $\theta = 0°$ to $\theta = 51°$, λ_C could be tuned from 563 nm to 510 nm. Angles $\theta > 51°$ could not be used, because parts of the parallel beam would have passed by the filters, which were only available in the size stated. λ_{SB} varied only by a small amount: the average bandwidth over the tuning range equaled $\lambda_{SB} = 17.7$ nm (range: 17.3–18.1 nm).

B. Two filters

The capability of the filter unit to independently adjust λ_C and λ_{SB} is illustrated in Fig. 4. The transmission spectrum

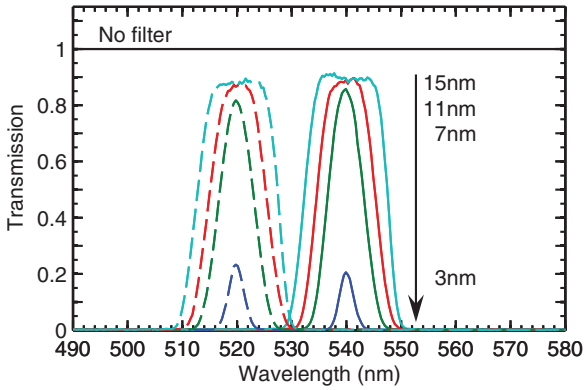

FIG. 4. The transmission spectrum with the two tunable thin-film filters is shown relative to the transmission spectrum without filters (solid black line). The two filters were rotated independently to transmit light only at the desired central wavelengths ($\lambda_C = 520$ nm and $\lambda_C = 540$ nm) with the desired bandwidths (3 nm $\leq \lambda_{SB} \leq$ 15 nm, 4 nm increments).

at 8 different angles of both filters is shown, yielding a transmitted central wavelength of 520 nm or 540 nm, at 4 different bandwidths from 3 nm to 15 nm. The maximum transmission remains nearly constant for $\lambda_{SB} \geq 9$ nm, but decreases for smaller bandwidths. For $\lambda_{SB} \geq 9$ nm, the maximum transmission efficiency was larger than 88% for $\lambda_C = 540$ nm and larger than 87% for $\lambda_C = 520$ nm, while for $\lambda_{SB} = 6$ nm, it was 81% for $\lambda_C = 540$ nm and 75% for $\lambda_C = 520$ nm.

For 5 bandwidths (3–15 nm), the bandwidth is plotted as a function of the central wavelength in Fig. 5, remaining virtually constant within the central wavelength range shown, demonstrating the ability to freely adjust the central wavelength at a given spectral bandwidth. However, the spectral tuning range of the central wavelength is limited by the bandwidth setting: the maximum rotation angle $\theta = 51°$ limits the pass-band shift of one filter to a minimal spectral position. To achieve a small total pass-band bandwidth, the other filter has to be rotated to an angle $\theta < 51°$, so that the central wavelength of the transmission pass-band of both filters increases with the bandwidth reduction, limiting the minimum achievable central wavelength at a given bandwidth. The same applies to the minimum rotation angle $\theta = 0°$, where the other filter is rotated to an angle $\theta > 0°$, decreasing the maximum achievable central wavelength at a given bandwidth. Therefore, for a bandwidth $\lambda_{SB} = 3$ nm, the tuning range was 522 nm $\leq \lambda_C \leq$ 555 nm, and for $\lambda_{SB} = 15$ nm, the range was 512 nm $\leq \lambda_C \leq$ 562 nm. Additionally, the quantitative evaluation of the transmitted intensity is shown in Fig. 5 for each bandwidth at the lowest and highest achievable central wavelength. In the bandwidth range 6 nm $\leq \lambda_{SB} \leq$ 15 nm, the transmitted intensity remains virtually constant for increased rotation angles. For the very small bandwidth $\lambda_{SB} = 3$ nm, the transmitted intensity is reduced by a factor of 3 for large rotation angles.

Finally, in Fig. 6, the transmitted intensity, i.e., the sum over all pixel values of the transmission spectrum, is plotted as a function of the bandwidth for 4 different central wavelengths, 520–550 nm. For all central wavelengths, essentially

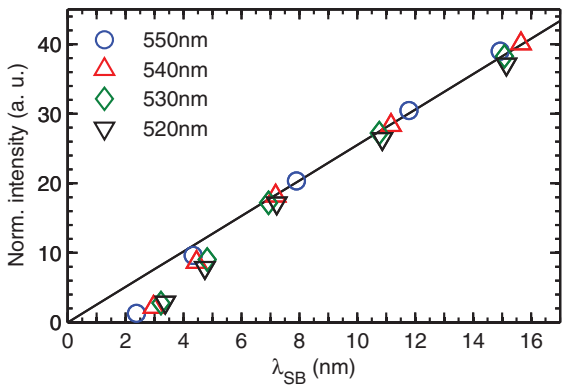

FIG. 6. The transmitted intensity, i.e., the sum over all pixel values of the transmission spectrum, is plotted as a function of the spectral bandwidth at four central wavelengths, in the range 520–550 nm. It is obvious that for a bandwidth $\lambda_{SB} > 6$ nm, the intensity increases linearly with the bandwidth, and for $\lambda_{SB} < 6$ nm with a larger slope.

the same characteristic was measured: for $\lambda_{SB} \geq 6$ nm, the intensity increases linearly with the bandwidth, while for $\lambda_{SB} < 6$ nm, the intensity drops to zero with a larger slope.

C. Fiber bundle

In Fig. 7(a), the spectrally filtered image of the fiber bundle, collimated using the collimating lens with f = 18 mm as illustrated in Fig. 1(b), is shown. The filters were set to

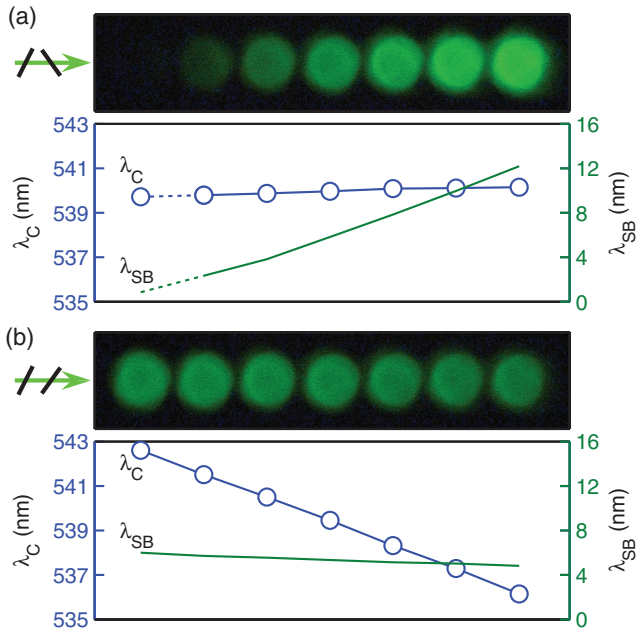

FIG. 7. The images of light transmitted through a linearly arranged fiber bundle focused onto a diffusing screen according to the setup in Fig. 1(b) is shown, for (a) counter-directional and (b) equidirectional rotating filters. The position-dependent central wavelength λ_C and bandwidth λ_{SB} of the filtered spectrum is shown for both cases. In (a), the central wavelength λ_C remained virtually constant (range: 539.8–540.1 nm), while the bandwidth λ_{SB} varied spatially (range: 2.3–12.2 nm). For the outermost left fiber, the transmitted intensity was too low for evaluation, so the bandwidth and central wavelength is indicated only by extrapolating the neighboring values. In (b), the central wavelength λ_C varied spatially (range: 542.6–536.1 nm), while the bandwidth λ_{SB} varied only by a smaller amount (range: 6.0–4.7 nm).

counter-directional rotation angles, +26.8° and −35.7°, respectively, yielding a central wavelength $\lambda_C = 540$ nm and a spectral bandwidth $\lambda_{SB} = 6$ nm for the center fiber of the fiber bundle. In the image, it is obvious that for the outermost left fiber virtually no light was transmitted, while for the outermost right fiber, the intensity was larger than for the central fiber. Below the image in Fig. 7(a), the filtered spectrum is shown for each single fiber. While λ_C remained virtually constant for all fibers (range: 539.8–540.1 nm), λ_{SB} varied spatially in the range 2.3–12.2 nm. Due to the low transmitted intensity, the first fiber was excluded from this evaluation, and is only indicated by extrapolation of the neighboring values.

In Fig. 7(b), the two filters were set to equidirectional rotation angles, +26.8° and +35.7°, respectively. Here, the intensity variations observed in the fiber images are considerably lower. However, the evaluation of the transmitted spectrum shows that, in contrast to counter-directional rotation, λ_C varied spatially (range: 542.6–536.1 nm), while λ_{SB} showed only a low variation (range: 6.0–4.7 nm). The same behavior was found for other central wavelengths of the central fiber, 520 nm, 530 nm, and 550 nm. The quantitative evaluation of the minimum and maximum central wavelength and bandwidth of the 7 fibers for counter- and equidirectional rotation and for the different central wavelengths is shown in Table I. In addition, the results of the same measurements, performed with a collimating lens with a focal length of f = 27 mm, are shown in Table I. Essentially, the following result was observed: for a decreasing central wavelength which equals an increasing rotation angle, the variations observed between the different fibers became larger, namely, bandwidth variations for counter-directional rotation and central wavelength variations for equidirectional rotation. For example, for counter-directional rotation with the central wavelength set to 520 nm for the central fiber, the bandwidth varied from 2.2 nm to 13.1 nm (=10.9 nm variation), while for the central wavelength 550 nm of the central fiber, the bandwidth varied only from 2.8 nm to 10.9 nm (=8.1 nm variation). On the other hand, for equidirectional rotation, the central wavelength varied for the 520 nm central fiber setting from 516.3 nm to 523.6 nm (=7.3 nm variation), while it varied only from 546.8 nm to 551.9 nm (=5.1 nm variation) for the 550 nm wavelength setting. When using the collimating lens with larger focal length (f = 27 mm instead of f = 18 mm), in all cases, the observed variations became smaller, namely, bandwidth variations for counter-directional rotation, and central wavelength variations for equidirectional rotation.

IV. DISCUSSION

In this study, we demonstrated a cost-effective optical filter unit that allows for fast and independent adjustment of the central wavelength in the range 522–555 nm and of the spectral bandwidth in the range 3–16 nm. Images can be filtered without requiring a scanning unit. The filter unit offers potential replacement for expensive light sources such as tunable lasers in devices where a spectral bandwidth larger than 3 nm is acceptable.

TABLE I. Minimum and maximum transmitted central wavelength λ_C and bandwidth λ_{SB} for each of the 7 fibers of the fiber bundle at different central wavelengths.

			$\lambda_C = 550$ nm[a]		$\lambda_C = 540$ nm		$\lambda_C = 530$ nm		$\lambda_C = 520$ nm	
			C[b]	E[b]	C	E	C	E	C	E
Lens 1[c]	λ_C	Min	549.6	546.8	539.8	536.1	529.9	525.7	519.8	516.3
f = 18 mm		Max	550.4	551.9	540.1	542.6	530.0	532.8	520.0	523.6
	λ_{SB}	Min	2.8	4.1	2.3	4.8	2.2	4.7	2.2	6.1
		Max	10.9	6.3	12.2	6.0	12.6	5.2	13.1	6.2
Lens 2[c]	λ_C	Min	549.6	548.6	539.7	537.9	529.8	527.8	519.9	517.7
f = 27 mm		Max	550.3	551.8	540.1	542.1	530.0	532.4	519.9	522.5
	λ_{SB}	Min	3.1	6.1	2.7	6.4	2.4	6.6	2.5	7.3
		Max	9.6	7.3	10.6	6.9	10.8	6.8	11.6	7.5

[a]Filter angles were adjusted so that the image of the central fiber showed the indicated central wavelength and a bandwidth of 6 nm for counter-directional rotation of the filters.
[b]Counter-directional rotation of the filters ("C") and equidirectional rotation of the filters ("E").
[c]For the collimating lens 1 (f = 18 mm), the first fiber was not evaluated, for the collimating lens 2 (f = 27 mm), all fibers were evaluated.

The measurements using one tunable optical band-pass filter (561/14 nm VersaChrome, Semrock, Inc., Rochester, NY, USA) show that the central wavelength can be adjusted by rotating the filter as predicted by Eq. (1). The tuning range is limited by the geometry of the filter, as the projected filter area apparent to the collimated beam of light is reduced by rotating the filter. The pass-band edges are flattened at increasing θ by 3.2 nm, which can be assumed to be due to the remaining divergence of the collimated beam of light, which has a larger influence at larger θ, because of the stronger wavelength-dependency. The filter transmission remains well above 90% for the whole tuning range, indicating a negligible influence of incident light polarization. These filters are therefore potentially useful for high-intensity illumination systems filtering unpolarized white light or for highly efficient fluorescence detection systems.

Two successively arranged optical band-pass filters were used to allow for simultaneous adjustment of the transmitted central wavelength and bandwidth, which is achieved by spectral overlap of the two pass-bands that are shifted against each other by rotating the filters independently to different angles. We showed that in the described setup, the spectral bandwidth can be freely adjusted in the range 3–16 nm, with the tuning range of the central wavelength depending on the desired bandwidth, e.g., 522–555 nm for $\lambda_{SB} = 3$ nm and 512–562 nm for $\lambda_{SB} = 15$ nm. However, when using different filter combinations, in principle the complete visible wavelength range can be covered.[5] The adjustable bandwidth range agrees well with the one reported by Jeong *et al.*,[19] where a tuning range of 4–17.4 nm was achieved, however using a point-like source instead of the 1500 μm diameter fiber used in this study. Additionally, we showed in this study that the transmitted intensity decreases only linearly with the bandwidth for $\lambda_{SB} \geq 6$ nm, thus allowing optical filtering with a high transmission efficiency >75%, which indicates that the proposed arrangement of two tunable thin-film optical band-pass filters can be used without significant transmission efficiency loss compared to the one-filter setup. Especially, for high-intensity illumination systems, the proposed filter unit is superior to commonly used diffraction based monochromators, which show a decreasing maximum transmission efficiency at decreasing bandwidth, resulting in a decrease of the transmitted intensity by the square of the bandwidth.[1] However, for $\lambda_{SB} < 6$ nm, the maximum transmission efficiency of the proposed filter unit decreases as well. This decline can be attributed to the non-perfect parallelism of the collimated beam of light, which reduces the transmission pass-band edge steepness of each filter. Consequently, the total transmission efficiency is reduced if the filter pass-bands only overlap in the spectral range of the edges, thus limiting its use for very small spectral bandwidths. This problem cannot be overcome easily, as it requires either a source with smaller diameters, e.g., point-source like,[19] which may not be available as a high intensity non-coherent light source, or a larger focal width of the collimating lens, which is also not always applicable due to the usually high numerical aperture of the source, which would then result in a low transmission efficiency. Also, the filter dimensions restrict the beam diameter and therefore the collimating lens diameter, which limits the focal length at a given numerical aperture. Due to the size of the filters and the need to independently rotate them by $\theta < 60^\circ$, the optical length of the filter unit theoretically has a lower limit of 62 mm to avoid collision of the rotated filters, which cannot be reduced without using smaller filters which would further restrict the beam diameter. The time required for switching between different filter settings is limited by the speed of the stepper motors driving the filter rotation, and was 400 ms for switching from lowest to highest rotation angle, and accordingly less for smaller spectral shifts, with a response time of less than 8 ms/nm. The parallel beam shift occurring during the propagation of the collimated beam through the filter unit can be minimized by rotating the filters into opposite directions. By focusing the collimated beam, the large beam shift can also be eliminated.[19] In such applications, equidirectional filter rotation can be used as well.

By showing spectrally filtered images of a linearly arranged fiber bundle, Fig. 7, we demonstrated the applicability of the filter unit to filtering images. The transmitted spectrum depends on the position within the image plane, along the axis perpendicular to the rotation axis of the filters. By rotating the filters in opposite directions, the central bandwidth is constant within the image along the axis perpendicular

to the filter rotation axis, but the bandwidth varies, e.g., 2–13 nm at the constant central wavelength of 540 nm, thereby producing intensity variations within the image. In contrast, by rotating the filters in the same direction, the bandwidth and therefore the intensity remains nearly constant along this axis, but the central wavelength shifts, e.g., from 536 nm to 543 nm, while the bandwidth varies only in the range 5–6 nm. This behavior can be explained by the transmission spectrum of a single filter, Fig. 2: the non-parallel parts of the collimated beam pass through the first filter position-dependent at a larger (or smaller) angle of incidence than the filter rotation angle, which effectively shifts the transmitted spectrum to shorter (or longer) wavelengths for these non-parallel parts of the beam. If both filters are rotated in opposite directions, the transmission pass-band of the second filter is shifted in the opposite direction; if they are rotated in the same direction, the transmission pass-band of the second filter is shifted in the same direction. Therefore, for counter-directional rotation, the total transmission bandwidth narrows for the non-parallel parts of the collimated beam due to a shift of the filter pass-bands in opposite directions, and for equidirectional rotation, the central wavelength shifts due to the pass-bands' shift in the same direction. The results confirm that this effect is more pronounced for decreasing central wavelengths, which is equivalent to increasing rotation angles, because the filter pass-bands shift by a larger amount at larger angles of incidence for a constant divergence angle. Compare Fig. 3 and Eq. (1), where the slope of the central wavelength function is larger for larger filter rotation angles. By using a longer focal length of the collimating lens, e.g., 27 mm instead of 18 mm, the non-parallel parts of the beam show a smaller divergence angle, which reduces the position-dependency of the transmitted central wavelength or spectral bandwidth in the image. For an even longer focal length, f = 80 mm, Iga *et al.*[12] filtered an image in a similar setup and varied the bandwidth from 1.5 nm to 3 nm, however, without specifying the position-dependency of the bandwidth or central wavelength within the image. For imaging systems, if this problem is predominant, e.g., when using a small focal length, this problem could be addressed by using equidirectional rotation of the filters, and by successively taking pictures while sweeping the filter unit over the tuning range at the desired bandwidth. In each picture, different parts can be assumed to be associated with different central wavelengths but identical bandwidth. We hypothesize that a composite picture with defined central wavelength and bandwidth could be reconstructed from this stack of pictures. Nevertheless, a careful specification of the position-dependent transmission characteristic of the filter unit is mandatory.

V. CONCLUSION

We conclude that tunable thin-film optical band-pass filters can be used for illumination systems with high wavelength tuning speed, where high intensities at small spectral bandwidths (3–16 nm) are required, if the tuning range (e.g., 522–555 nm) is sufficient for the application or it is acceptable to replace the filters to cover the whole visible spectral range. Spectral filtering of images or fiber bundles without a scanning unit is possible, which may be useful for imaging systems like microscopes or endoscopes, but may be limited by the divergence of the collimated beam. Careful specification of the filter unit in the imaging system is recommended.

ACKNOWLEDGMENTS

The authors thank Mr. Thomas Pongratz for technical support and Mr. Sebastian Fiedler for assistance during the measurements.

[1] J. R. Lakowicz, *Principles of Fluorescence Spectroscopy* (Springer, New York, 2006), p. 27.
[2] Y. Garini, I. T. Young, and G. McNamara, Cytometry, Part A **69A**, 735 (2006).
[3] P. Prabhat, N. Anderson, and T. Erdogan, Semrock White Paper Series (Semrock, Inc., 2012), see http://www.semrock.com/spectral-imaging-with-versachrome.aspx.
[4] M. Czerny and A. F. Turner, Z. Phys. **61**, 792 (1930).
[5] T. Erdogan and L. Wang, Semrock White Paper Series (Semrock, Inc., 2010), see http://www.semrock.com/semrock-versachrome-tunable-bandpass-filters.aspx.
[6] E. Dekemper, N. Loodts, B. Van Opstal, J. Maes, F. Vanhellemont, N. Mateshvili, G. Franssens, D. Pieroux, C. Bingen, C. Robert, L. De Vos, L. Aballea, and D. Fussen, Appl. Opt. **51**, 6259 (2012).
[7] P. E. Buchsbaum and J. D. Lane, "Tunable variable bandpass optical filter," U.S. patent 6,700,690 (2 March 2004).
[8] A. Emadi, H. Wu, G. de Graaf, P. Enoksson, J. H. Correia, and R. Wolffenbuttel, Appl. Opt. **51**, 4308 (2012).
[9] S. T. Wu, Appl. Opt. **28**, 48 (1989).
[10] S. C. Gebhart, R. C. Thompson, and A. Mahadevan-Jansen, Appl. Opt. **46**, 1896 (2007).
[11] Y. H. Chen, C. T. Wang, C. P. Yu, and T. H. Lin, Opt. Express **19**, 25441 (2011).
[12] M. Iga, N. Kakuryu, T. Tanaami, J. Sajiki, K. Isozaki, and T. Itoh, Rev. Sci. Instrum. **83**, 103707 (2012).
[13] M. Mitov, Adv. Mater. **24**, 6260 (2012).
[14] S. Furumi, S. Yokoyama, A. Otomo, and S. Mashiko, Appl. Phys. Lett. **84**, 2491 (2004).
[15] Y. Huang and S. Zhang, Opt. Lett. **36**, 4563 (2011).
[16] Y. Huang and S. Zhang, Appl. Opt. **51**, 5780 (2012).
[17] A. Chanishvili, G. Chilaya, G. Petriashvili, R. Barberi, R. Bartolino, G. Cipparrone, A. Mazzulla, and L. Oriol, Appl. Phys. Lett. **83**, 5353 (2003).
[18] H. P. Yu, B. Y. Tang, J. H. Li, and L. Li, Opt. Express **13**, 7243 (2005).
[19] H. J. Jeong, J. W. Ahn, D. Do, and D. G. Gweon, Rev. Sci. Instrum. **83**, 093705 (2012).